ACS APPLIED MATERIALS & INTERFACES

Letter

www.acsami.org

Enhanced Non-Endocytotic Uptake of Mesoporous Silica Nanoparticles by Shortening the Peptide Transporter Arginine Side Chain

Cheng-Hsun Wu,† Yi-Ping Chen,† Si-Han Wu, Yann Hung, Chung-Yuan Mou,* and Richard P. Cheng*

Department of Chemistry, National Taiwan University, Taipei 10617, Taiwan

Supporting Information

ABSTRACT: Mesoporous silica nanoparticles (MSNs) are multifunctional nanocarriers with potential biomedical applications. However, MSNs are frequently trapped in endosomes upon cellular uptake through endocytosis, requiring endosomal escape. Herein, enhanced nonendocytosis was observed for 300 nm MSNs by conjugating peptides with noncanonical arginine analogs.

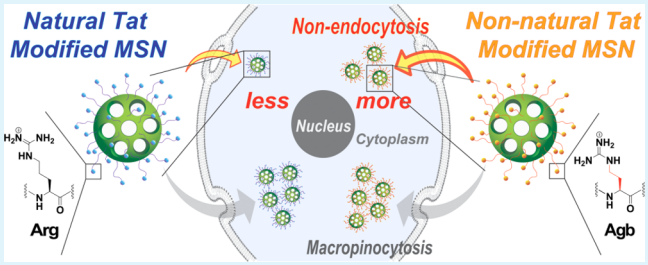

KEYWORDS: *mesoporous materials, non-natural peptides, arginine analogs, cellular uptake, nonendocytosis*

1. INTRODUCTION

Nanoparticles are impressive carriers for delivering bioactive small molecules and biomacromolecules (peptides, proteins, RNAs, DNAs, etc.) across the cell membrane.[1,2] Although nanoparticles can enter cells,[1,3−5] they are frequently trapped in intracellular vesicles such as endosomes and lysosomes,[6,7] hampering the development for biomedical applications. One strategy to facilitate endosomal escape is surface conjugation with either cationic polymer polyethylenimine[8] or cell-penetrating peptides;[9] however, enhanced nonendocytotic uptake would be even more desirable to circumvent the endosome/lysosome altogether.[7,9]

Mesoporous silica nanoparticles (MSNs) have emerged as a widely used nanocarrier for biological applications[6,10] and potential drug delivery systems.[11,12] For the various MSN sizes, small size MSNs (50 to 100 nm in diameter) have the highest cellular uptake efficiency,[13,14] which has been attributed to clathrin-mediated endocytosis.[15] However, the development of medium size MSNs (∼ 300 nm in diameter) has been limited because of the lack of efficient cellular uptake.[13] The limited delivery of medium size MSNs to the cytoplasm has been mentioned in a few studies with undetermined uptake mechanism.[16]

The cell-penetrating peptide derived from human immunodeficiency virus transactivator of transcription protein (Tat) has been conjugated to nanoparticles to enhance cellular uptake mostly through endocytosis,[7,17] with low cytotoxicity and enhanced endosomal escape (after endocytosis).[9] Also, Tat-derived peptides have been conjugated to different cargoes to enable cellular uptake via macropinocytosis,[18] which is a form of endocytosis. Tat-derived peptides alone can translocate across the cell membrane through nonendocytotic energy-independent pathways,[19] which has been mostly attributed to direct transduction.[20−26] This nonendocytotic uptake of Tat-derived peptides is mediated by the dense packing of cationic guanidinium groups,[25] which form multiplex interactions with lipid head groups and cytoskeleton to form topologically active saddle-splay membrane curvature for pore formation and membrane permeabilization.[25] One determining factor for generating saddle-splay membrane curvature is the spacing between guanidinium groups and the rigidity of the presentation.[26] As such, altering the spacing between the guanidinium groups should affect uptake efficiency. Indeed, shortening the Arg side chain length by one methylene for all six Arg residues in Tat-derived peptides enhanced the cellular uptake.[19] Also, temperature dependence studies suggested nonendocytotic uptake for these peptides bearing noncanonical Arg analogs.[19] Retaining this uptake behavior upon conjugating these peptides onto comparatively large nanoparticles would be highly desirable. However, the drastic difference in overall characteristics between peptide alone and peptide-conjugated nanoparticles may result in difference in uptake behavior. Nevertheless, Tat-derived peptides containing noncanonical Arg analogs were conjugated onto 300 nm MSNs to affect the uptake efficiency and expand the uptake routes (to beyond endocytosis).

2. RESULTS AND DISCUSSION

Tat-derived peptides with noncanonical Arg analogs were conjugated onto medium size (300 nm) MSNs (Chart 1). All six Arg residues in the Tat-derived peptide (ArgTat) were simultaneously replaced with the Arg analogs Agh (one

Received: September 16, 2013
Accepted: November 15, 2013
Published: November 21, 2013

Chart 1. Sequences of Natural Tat and Tat-Derived Peptides

Natural Tat(48-57)
-Gly-Arg-Lys-Lys-Arg-Arg-Gln-Arg-Arg-Arg-

XaaTat peptides
AghTat: Ac-Cys-Gly-Agh-Lys-Lys-Agh-Agh-Gln-Agh-Agh-Agh-NH_2
ArgTat: Ac-Cys-Gly-Arg-Lys-Lys-Arg-Arg-Gln-Arg-Arg-Arg-NH_2
AgbTat: Ac-Cys-Gly-Agb-Lys-Lys-Agb-Agb-Gln-Agb-Agb-Agb-NH_2

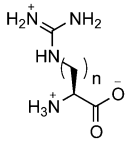

n = 4, Agh, (*S*)-2-amino-6-guanidinohexanoic acid
3, Arg, L-arginine
2, Agb, (*S*)-2-amino-4-guanidinobutyric acid

methylene longer than Arg) or Agb (one methylene shorter than Arg) (Chart 1). Peptides containing these noncanonical Arg analogs showed higher resistance against proteolysis compared to the corresponding Arg-containing peptides.[27] This higher protease resistance should enhance the availability of the peptides in the endosome and lysosome to mediate endosomal escape. Shortening the Arg side chain length should shorten the distance between neighboring guanidinium groups and facilitate the formation of saddle-splay membrane curvature for pore formation and membrane permeabilization.[25] A cysteine residue was added at the N-terminus to enable conjugation onto the MSNs (Chart 1).

The APTMS-FITC-functionalized MSNs were synthesized by co-condensation with FITC (fluorescein isothiocyanate) coupled to the amino group of 3-aminopropyl-trimethoxysilane (APTMS) (Scheme 1). To enable conjugation to the peptides, we introduced an amine-to-sulfhydryl cross-linker *N*-(*α*-maleimidoacetoxy) succinimide ester (AMAS). The succinimide ester was coupled to the primary amine on the MSN and the maleimide group was reacted with the thiol group on the Cys residue of the Tat-derived peptides. The average weight percent of APTMS functionalized onto the nanoparticles was 2.3 wt % as determined by elemental analysis. The average weight percent of AMAS attached to MSN (containing APTMS) was 8.8 wt % as determined by thermogravimetric analysis; the theoretical maximum coverage would be 18.4 wt %. The amount of peptide conjugation onto AMAS-MSNs was 3.3×10^{-4} mol/g based on the UV−vis absorbance of the reaction supernatant for a related Tat-derived peptide with the same immediate sterics surrounding the linking Cys residue as the experimental peptides (ArgTat, AgbTat, and AghTat). Since the overall charge of the experimental peptides is the same, the conjugation efficiency should be similar for the different experimental peptides. Transmission electron microscopy (TEM) showed an average diameter of 300 nm for the MSNs with uniform pore structure before and after functionalization with APTMS, coupling of AMAS, and conjugation with the Tat-derived peptides (see Figure S2 in the Supporting Information). The XaaTat-MSN formed stable homogeneous suspensions, most likely due to the mutual repulsion between the highly positively charged MSNs.

The effect of the Tat-derived peptides on the uptake of MSNs into HeLa cells was investigated by flow cytometry. After incubation with the nanoparticles or spheres, the HeLa cells were washed and detached from the dish by trypsinization. The extracellular fluorescence quencher trypan blue was then added to the cell suspension to quench the fluorescence from the remaining MSNs adsorbed onto the exterior surface of the cells.[2,28,29] The intracellular fluorescence in live cells was then determined by flow cytometry to assess the amount of cellular uptake (see Figure 1A and Figures S4, S5, and S8A in the Supporting Information). Because fluorescence from the cytoplasm and the endosome/lysosome cannot be distinguished, the flow cytometry data was reported in percent cellular uptake (Figure 1A). Cells with fluorescence higher than

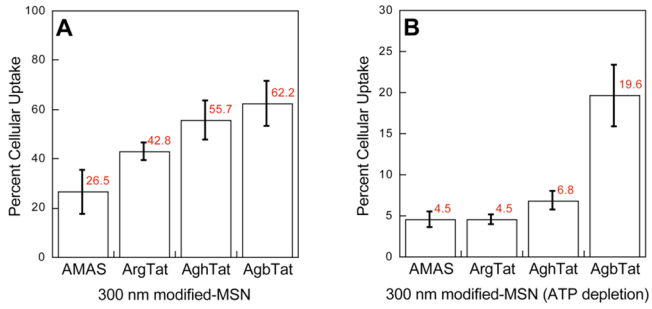

Figure 1. Cellular uptake into HeLa cells for 300 nm AMAS-MSN and XaaTat-MSNs in the (A) absence and (B) presence of ATP inhibitors sodium azide and 2-deoxy-D-glucose.

Scheme 1. (A) Synthesis and Surface Functionalization of MSNs, followed by (B) Conjugation with Tat-Derived Peptides

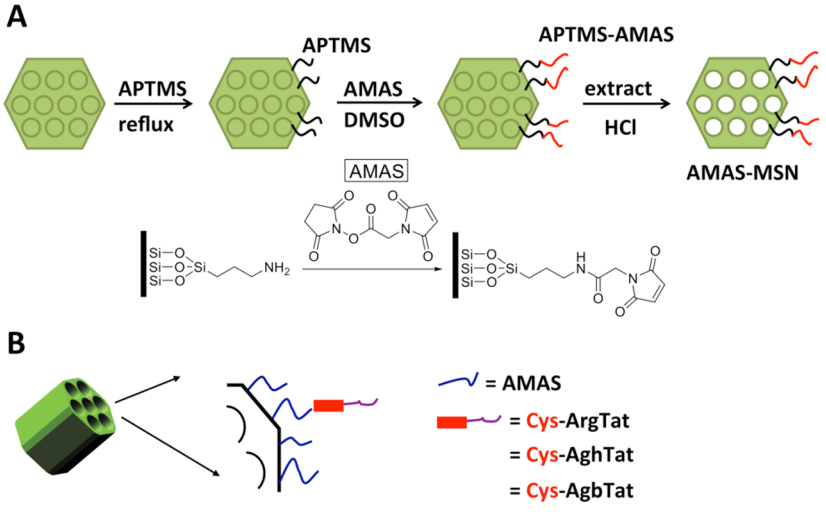

dx.doi.org/10.1021/am4039882 | *ACS Appl. Mater. Interfaces* 2013, 5, 12244−12248

the maximum fluorescence of live control cells were considered to exhibit MSN uptake (see Figure S5 in the Supporting Information). The percent cellular uptake of the wild type Tat peptide-modified MSN, ArgTat-MSN, was significantly higher than the control nanoparticle AMAS-MSN (Figure 1A).[17] The MSNs conjugated with the two Tat-derived peptides containing non-natural Arg analogs, AghTat-MSN and AgbTat-MSN, had even higher percent cellular uptake compared to ArgTat-MSN (Figure 1A). Under these conditions, the cellular uptake of XaaTat-MSN could occur via both endocytotic and non-endocytotic pathways.[4,30] To inhibit endocytosis (and thus macropinocytosis), cells were treated with ATP inhibitors sodium azide and 2-deoxy-D-glucose,[5,31−35] and then incubated with the various MSNs in the presence of both ATP inhibitors. Under this ATP depleted condition, energy-dependent endocytotic pathways were blocked,[31,32] and uptake was significantly reduced for live cells (Figure 1B and Figure S8B in the Supporting Information). This suggests that the enhanced uptake of the MSNs upon conjugating the Tat peptides mostly occurred through endocytosis/macropinocytosis. Importantly, 20% of the cells still showed uptake of AgbTat-MSN even upon inhibition of endocytosis (Figure 1B), suggesting that a portion of the AgbTat-MSNs crossed the cell membrane through energy-independent nonendocytotic pathways such as direct transduction.

Distribution of XaaTat-MSNs in live HeLa cells was analyzed qualitatively by confocal microscopy (Figure 2). The MSNs were cocultured with FM 4−64 (red), which is an endosome tracker.[36−40] The AMAS-MSNs exhibited punctate cytoplasmic distribution patterns (Figure 2, top row, left panel). AMAS-MSN (green for FITC) predominantly colocalized with the FM 4−64 (red) in live cells, resulting in yellow spots in the merged images (Figure 2, top row, right panel). As such, AMAS-MSN was mostly trapped in endosome or lysosome vesicles, consistent with literature reports that MSN uptake occurs through endocytosis.[2,15] In contrast, the merged image for ArgTat-MSN showed both green and yellow spots (Figure 2, second row, right panel). Importantly, there were more FITC green spots in the merged image for ArgTat-MSN compared to that for AMAS-MSN. This demonstrates that ArgTat enhanced the delivery of MSNs into the cytoplasm by endosomal escape or nonendocytotic pathways, consistent with reports on enhanced access to the cytoplasm (opposed to trapped in the endosome) upon conjugating Tat peptide to nanoparticles.[19,41] The merged images of AghTat-MSN and AgbTat-MSN displayed significantly more green spots distributed in the live cells compared to ArgTat-MSN (Figure 2), showing enhanced access to the cytoplasm mediated by AghTat and AgbTat.

Flow cytometry data showed that conjugating ArgTat onto 300 nm MSN increased overall uptake but not nonendocytotic uptake (Figure 1 and Figure S8 in the Supporting Information). However, confocal microscopy showed that ArgTat increased the distribution of 300 nm MSN in the cytoplasm (Figure 2), suggesting that ArgTat enhanced the efficiency of endocytotic uptake and endosomal escape. The overall uptake for AghTat-MSN was slightly higher than that for ArgTat-MSN (Figure 1A). Also, the nonendocytotic uptake of AghTat-MSN was only marginally higher than that of ArgTat-MSN (Figure 1B). However AghTat clearly enabled more MSN uptake into the cytoplasm compared to ArgTat based on observations by confocal microscopy (Figure 2), suggesting more efficient endocytotic uptake and endosomal escape mediated by AghTat compared to ArgTat. Similar to AghTat, AgbTat mediated

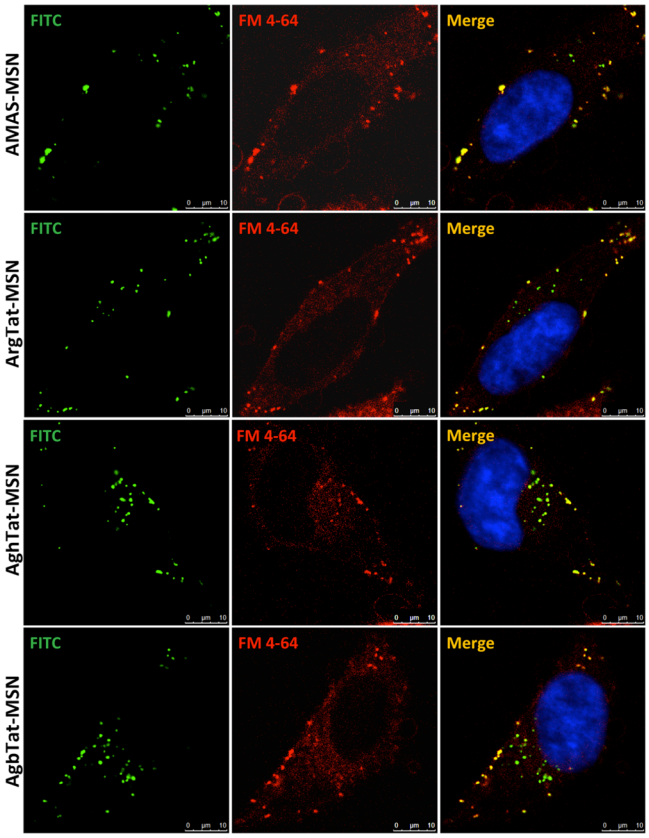

Figure 2. Confocal microscopy images of 300 nm AMAS-MSN and XaaTat-MSNs in live unfixed HeLa cells (left column), cotreated with the endosome-specific marker FM 4−64 (center column), and stained with the DNA-specific DAPI to obtain the merged endosomal colocalization images (right column). The MSNs are green, FM 4−64-labeled endosomes are red, DAPI is blue, colocalized MSNs and endosomes are yellow.

significant MSN uptake into the cytoplasm (Figure 2). In contrast to AghTat, AgbTat significantly enhanced membrane translocation through nonendocytotic pathways (Figure 1B), although access to the cytoplasm through endosomal escape cannot be completely ruled out. Increased endosomal escape mediated by AghTat and AgbTat compared to ArgTat could be due to enhanced resistance to proteolytic degradation of peptides containing the noncanonical Arg analogs[27] in the endosome/lysosome to enable endosomal escape. Increased nonendocytotic uptake mediated by AgbTat (Figure 1B) is consistent with the intended design of shortening the spacing between neighboring guanidinium groups to provide a more rigid presentation of the guanidinium groups for the formation of saddle-splay membrane curvature and permeabilization of the membrane.[26] Furthermore, these peptide conjugated medium sized MSNs exhibited minimal cytotoxicity up to 50 μg/mL based on WST assays (see Figure S9 in the Supporting Information), suggesting that such nanoparticles should be suitable for biomedical applications.

Preliminary studies on small sized MSNs (50 nm) and large sized mesoporous silica spheres (MSSs) (1 μm) in the absence and presence of peptide conjugation were also performed (see Figure S10 in the Supporting Information), to further explore the utility of the Tat-derived peptides with noncanonical Arg analogs for enhancing uptake through nonendocytotic pathways. The three peptides conjugated to 50 nm MSNs exhibited

similar relative cellular uptake under ATP-depleted conditions (see Figure S10A in the Supporting Information). This uptake was slightly higher than that for the control AMAS-MSN. However, peptide conjugation onto large 1 μm MSSs did not alter cellular uptake under ATP-depleted conditions (see Figure S10B in the Supporting Information). This variation in uptake behavior for the peptide-conjugated small size MSNs (50 nm), medium size MSNs (300 nm), and large size MSSs (1 μm) is consistent with previous reports showing size dependence in cellular uptake efficiency and mechanism of the MSNs.[1,13] The difference in uptake behavior for the different sized MSNs upon conjugating the peptides may be due to difference in surface curvature and thus guanidinium group presentation. This would affect the interaction with cell surface negatively charged moieties, which is critical for cellular uptake. The size dependence on enhanced uptake and uptake mechanism remains to be fully investigated. Nonetheless, enhanced nonendocytotic uptake has been achieved for medium-sized MSNs (300 nm) by conjugating Tat-derived peptides bearing noncanonical Arg analogs with shortened side chain length.

3. CONCLUSION

In this study, Tat-derived peptides containing noncanonical Arg analogs were conjugated onto medium-sized MSNs (300 nm) and the cellular uptake efficiency was enhanced with increased access to the cytoplasm. Furthermore, endosomal trapping of the 300 nm MSN was partially circumvented by improving the efficiency of endosomal escape and even enhancing uptake through nonendocytotic pathways by introducing noncanonical Arg analogs with varying side chain lengths. Therefore, rational surface design that alters the presentation of guanidinium groups on nanoparticles is a viable strategy to enhance desirable uptake properties for biomedical applications.

■ ASSOCIATED CONTENT

Supporting Information

Experimental data for synthesis, characterization, and biological experimental methods; TEM images of 50 nm MSNs, 300 nm MSNs, and 1 μM MSSs; flow cytometry results of 50 nm MSNs and 1 μm MSSs; the cell viability results for 300 nm MSNs. This material is available free of charge via the Internet at http://pubs.acs.org.

■ AUTHOR INFORMATION

Corresponding Authors

*E-mail: rpcheng@ntu.edu.tw.
*E-mail: cymou@ntu.du.tw.

Author Contributions

†C.-H.W. and Y.-P.C. contributed equally.

Notes

The authors declare no competing financial interest.

■ ACKNOWLEDGMENTS

This work was supported by National Taiwan University (R.P.C. and C.Y.M.) and the National Science Council in Taiwan (RPC, NSC-99-2113-M-002-002-MY2 and NSC-101-2113-M-002-006-MY2).

■ REFERENCES

(1) Zhao, F.; Zhao, Y.; Liu, Y.; Chang, X. L.; Chen, C. Y.; Zhao, Y. L. *Small* **2011**, *7*, 1322−1337.
(2) Slowing, I. I.; Vivero-Escoto, J. L.; Wu, C.-W.; Lin, V. S.-Y. *Adv. Drug Delivery Rev.* **2008**, *60*, 1278−1288.
(3) Rejman, J.; Oberle, V.; Zuhorn, I. S.; Hoekstra, D. *Biochem. J.* **2004**, *377*, 159−169.
(4) Slowing, I.; Trewyn, B. G.; Lin, V. S.-Y. *J. Am. Chem. Soc.* **2006**, *128*, 14792−14793.
(5) Meng, H.; Yang, S.; Li, Z. X.; Xia, T.; Chen, J.; Ji, Z. X.; Zhang, H. Y.; Wang, X.; Lin, S. J.; Huang, C.; Zhou, Z. H.; Zink, J. I.; Nel, A. E. *ACS Nano* **2011**, *5*, 4434−4447.
(6) Vivero-Escoto, J. L.; Slowing, I. I.; Trewyn, B. G.; Lin, V. S.-Y. *Small* **2010**, *6*, 1952−1967.
(7) Torchilin, V. P. *Adv. Drug Delivery Rev.* **2008**, *60*, 548−558.
(8) Boussif, O.; Lezoualch, F.; Zanta, M. A.; Mergny, M. D.; Scherman, D.; Demeneix, B.; Behr, J. P. *Proc. Natl. Acad. Sci. U. S. A.* **1995**, *92*, 7297−7301.
(9) El-Sayed, A.; Futaki, S.; Harashima, H. *AAPS J.* **2009**, *11*, 13−22.
(10) Wu, S.-H.; Hung, Y.; Mou, C.-Y. *Chem. Commun.* **2011**, *47*, 9972−9985.
(11) Chen, C.; Geng, J.; Pu, F.; Yang, X.; Ren, J.; Qu, X. *Angew. Chem., Int. Ed.* **2011**, *50*, 882−886.
(12) Yang, X.; Liu, X.; Liu, Z.; Pu, F.; Ren, J.; Qu, X. *Adv. Mater.* **2012**, *24*, 2890−2895.
(13) Lu, F.; Wu, S.-H.; Hung, Y.; Mou, C.-Y. *Small* **2009**, *5*, 1408−1413.
(14) Gan, Q.; Dai, D. W.; Yuan, Y.; Qian, J. C.; Sha, S.; Shi, J. L.; Liu, C. S. *Biomed. Microdevices* **2012**, *14*, 259−270.
(15) Chung, T.-H.; Wu, S.-H.; Yao, M.; Lu, C.-W.; Lin, Y.-S.; Hung, Y.; Mou, C.-Y.; Chen, Y.-C.; Huang, D.-M. *Biomaterials* **2007**, *28*, 2959−2966.
(16) Slowing, I. I.; Trewyn, B. G.; Lin, V. S.-Y. *J. Am. Chem. Soc.* **2007**, *129*, 8845−8849.
(17) Mao, Z. W.; Wan, L.; Hu, L.; Ma, L.; Gao, C. Y. *Colloids Surf., B* **2010**, *75*, 432−440.
(18) Wadia, J. S.; Stan, R. V.; Dowdy, S. F. *Nat. Med.* **2004**, *10*, 310−315.
(19) Wu, C.-H.; Chen, Y.-P.; Mou, C.-Y.; Cheng, R. P. *Amino Acids* **2013**, *44*, 473−480.
(20) Thoren, P. E. G.; Persson, D.; Isakson, P.; Goksor, M.; Onfelt, A.; Norden, B. *Biochem. Biophys. Res. Commun.* **2003**, *307*, 100−107.
(21) Lundberg, P.; Langel, U. *J. Mol. Recognit.* **2003**, *16*, 227−233.
(22) Herce, H. D.; Garcia, A. E. *Proc. Natl. Acad. Sci. U.S.A.* **2007**, *104*, 20805−20810.
(23) Ter-Avetisyan, G.; Tuennemann, G.; Nowak, D.; Nitschke, M.; Herrmann, A.; Drab, M.; Cardoso, M. C. *J. Biol. Chem.* **2009**, *284*, 3370−3378.
(24) Schmidt, N.; Mishra, A.; Lai, G. H.; Wong, G. C. L. *FEBS Lett.* **2010**, *584*, 1806−1813.
(25) Mishra, A.; Lai, G. H.; Schmidt, N. W.; Sun, V. Z.; Rodriguez, A. R.; Tong, R.; Tang, L.; Cheng, J. J.; Deming, T. J.; Kamei, D. T.; Wong, G. C. L. *Proc. Natl. Acad. Sci. U.S.A.* **2011**, *108*, 16883−16888.
(26) Schmidt, N. W.; Lis, M.; Zhao, K.; Lai, G. H.; Alexandrova, A. N.; Tew, G. N.; Wong, G. C. L. *J. Am. Chem. Soc.* **2012**, *134*, 19207−19216.
(27) Izdebski, J.; Witkowska, E.; Kunce, D.; Oriowska, A.; Baranowska, B.; Wolinska-Witort, E. *J. Pept. Sci.* **2004**, *10*, 524−529.
(28) Hed, J.; Hallden, G.; Johansson, S. G. O.; Larsson, P. *J. Immunol. Methods* **1987**, *101*, 119−125.
(29) Moktan, S.; Rausher, D. *Int. J. Pept. Res. Ther.* **2012**, *18*, 227−237.
(30) Richard, J. P.; Melikov, K.; Vives, E.; Ramos, C.; Verbeure, B.; Gait, M. J.; Chernomordik, L. V.; Lebleu, B. *J. Biol. Chem.* **2003**, *278*, 585−590.
(31) Furuichi, K.; Ra, C.; Isersky, C.; Rivera, J. *Immunology* **1986**, *58*, 105−110.
(32) Schwoebel, E. D.; Ho, T. H.; Moore, M. S. *J. Cell Biol.* **2002**, *157*, 963−974.
(33) Potocky, T. B.; Menon, A. K.; Gellman, S. H. *J. Biol. Chem.* **2003**, *278*, 50188−50194.

(34) Sato, K.; Nagai, J.; Mitsui, N.; Yumoto, R.; Takano, M. *Life Sci.* **2009**, *85*, 800−807.
(35) Chae, S. Y.; Kim, H. J.; Lee, M. S.; Jang, Y. L.; Lee, Y.; Lee, S. H.; Lee, K.; Kim, S. H.; Kim, H. T.; Chi, S.-C.; Park, T. G.; Jeong, J. H. *Macromol. Biosci.* **2011**, *11*, 1169−1174.
(36) Vida, T. A.; Emr, S. D. *J. Cell Biol.* **1995**, *128*, 779−792.
(37) Betz, W. J.; Mao, F.; Smith, C. B. *Curr. Opin. Neurobiol.* **1996**, *6*, 365−371.
(38) Wiederkehr, A.; Avaro, S.; Prescianotto-Baschong, C.; Haguenauer-Tsapis, R.; Riezman, H. *J. Cell Biol.* **2000**, *149*, 397−410.
(39) Loudet, A.; Han, J.; Barhoumi, R.; Pellois, J.-P.; Burghardt, R. C.; Burgess, K. *Org. Biomol. Chem.* **2008**, *6*, 4516−4522.
(40) Kitakura, S.; Vanneste, S.; Robert, S.; Löfke, C.; Teichmann, T.; Tanaka, H.; Frimi, J. *Plant Cell* **2011**, *23*, 1920−1931.
(41) Coupland, P. G.; Briddon, S. J.; Aylott, J. W. *Integr. Biol.* **2009**, *1*, 318−323.